Optics Communications 352 (2015) 135–139

Contents lists available at ScienceDirect

Optics Communications

journal homepage: www.elsevier.com/locate/optcom

Angularly-resolved variable wave-retarder using light scattering from a thin metallic cylinder

Izcoatl Saucedo-Orozco [a,b], Rafael Espinosa-Luna [a,b,*], Qiwen Zhan [a]

[a] Electro-Optics Program, University of Dayton, 300 College Park, Dayton, OH 45469, USA
[b] GIPYS, Centro de Investigaciones en Óptica, A. C., Loma del Bosque 115, Colonia Lomas del Campestre, C. P. 37150 León, Guanajuato, Mexico

ARTICLE INFO

Article history:
Received 2 February 2015
Received in revised form
22 April 2015
Accepted 27 April 2015
Available online 30 April 2015

Keywords:
Physical optics
Scattering
Polarization
Cylinder
Variable wave-retarder

ABSTRACT

Experimental results show that the generation of spatially variable polarization states can be easily realized by using the light scattered from a thin metallic cylinder. The 360° angularly planar scattered light can be described as closed paths on the Poincarè sphere that connect antipodal polarizations. The simple experimental arrangement demonstrates that the thin metallic cylinder behaves as an angularly-resolved variable wave-retarder.

1. Introduction

The generation of polarization states has been always a very important theme in optics and photonics. For a long time, it has involved the use of conventional passive polarization optical devices, many of them based in the natural crystal birefringent properties of minerals, like the calcite-based linear polarizers or the mica and quartz-based retardation wave-plates. Recently, the use of electro-optic techniques has given rise to a lot of devices that induce phase changes in the electromagnetic field components (liquid crystal displays, liquid crystal on semiconductors, photoelastic modulators, Faraday rotators, among others). These modern devices are being used extensively in different basic research, applications, and even commercial areas [1–4]. There are many experimental possibilities to generate any polarization state on a beam emerging from a given light source, usually a collimated beam from a laser. Most methods employed to polarize light require the use of linear polarizers, half-, and quarter-wave retarder plates [5,6], where the wave plates generally are of the variable wave-retarder type. Once the beam has been polarized in the desired state, the generated polarized beam usually is handled properly to illuminate a sample under study, where the most common is the collimated geometry. Recently, the necessity to increase the polarization of light applications in science, engineering, and inspection areas has created opportunities to explore new forms to polarize light, where the method presented here could be a useful option [7–10]. In this work, we present experimental evidence that closed-paths on the Poincarè sphere can be generated and distributed angularly with the use of a thin metallic cylinder, illuminated under a planar geometry of incidence (incidence normal to the cylinder axis). The simple experimental arrangement reported here demonstrates that the thin metallic cylinder behaves as a passive angularly-resolved variable wave-retarder.

2. Theory

The polarization of light can be represented by the Stokes vector S in terms of the orthogonal components of the electric field vector (E_p, E_s) and their phase difference (δ), according to [6]

$$S = \begin{pmatrix} s_0 \\ s_1 \\ s_2 \\ s_3 \end{pmatrix} = \begin{pmatrix} E_p^2 + E_s^2 \\ E_p^2 - E_s^2 \\ 2E_p E_s \cos\delta \\ 2E_p E_s \sin\delta \end{pmatrix} \quad (1)$$

On the other hand, the normalized Stokes parameters can be displayed in a real three-dimensional space as a function of the azimuth ($0 \le 2\psi \le \pi/2$) and the ellipticity ($-\pi/2 \le 2\varepsilon \le \pi/2$) angles of the Poincarè sphere, respectively [6].

* Corresponding author at: GIPYS, Centro de Investigaciones en Óptica, A. C., Loma del Bosque 115, Colonia Lomas del Campestre, C. P. 37150 León, Guanajuato, Mexico.
E-mail address: reluna@cio.mx (R. Espinosa-Luna).

http://dx.doi.org/10.1016/j.optcom.2015.04.074
0030-4018/

$$S = s_0 \begin{pmatrix} 1 \\ \cos(2\varepsilon)\cos(2\psi) \\ \cos(2\varepsilon)\sin(2\psi) \\ \sin(2\varepsilon) \end{pmatrix} = \begin{pmatrix} 1 \\ s_1 \\ s_2 \\ s_3 \end{pmatrix} \tag{2}$$

2.1. Problem description

The scattering and diffraction of light by thin cylinders have been reported in both planar [11–14] and conical geometries of incidence [15,16]. Even when it is well known the scattered light is distributed on a plane perpendicular to the cylinder axis or on the surface of a cone, depending on whether the illuminating light incident perpendicularly to the cylinder axis or if it has a component along it, the precise polarization behavior associated with the incident polarization states is still unknown. The objective of this work is to show that the scattering of polarized light from a metallic cylinder can be used for a simple angularly-resolved variable wave-retarder.

3. Methods

The Fig. 1 shows the experimental setup employed. A collimated beam of light with 2 mm of beam size (HeNe laser, 632.8 nm) was generated and sent toward a metallic cylinder (electric guitar nickel string, with a 254 μm diameter). The cylinder was placed at the center of an automated rotation stage of an angle resolved scattering system (ARS; Oriel goniometer, with stepper motors), which is able to measure the polarized scattered light at each scattering angle θ_s, from $0° \le \theta_s \le 360°$. The scattered light lies within a plane surface perpendicular to the cylinder axis. A set of six incident polarization states (linear horizontal or *p*, perpendicular or *s*, to +45° and to −45°, and circular right- and left-handed polarization states, respectively) were generated using a polarization state generator (PSG) and each of them were analyzed employing a polarization state analyzer (PSA). A PSG was used with a Glan–Thompson linear polarizer (Thorlabs, GTH10M) followed by a liquid crystal variable retarder (Thorlabs, LCC1111-A and LCC25 controller), each mounted on motorized rotations stages (Thorlabs, PRM1Z8E). The PSA employed is a commercial polarimeter (Thorlabs, PAX5710VIS-T), consisting of a head, a controller and a software program that allows the automated detection of the scattered Stokes vector. The head contains an achromatic rotating quarter-wave plate, a linear polarizer and a photodetector. The scattered Stokes vectors were measured every 1° and were plotted by interpolating data with 6° step, except around 0° (where the PSA is rotated and placed between the PSG and the cylinder, obstructing the incident light) and 180° (where a slight saturation occurs at the photodetector), respectively.

The incident linear s- and p-polarization states are scattered uniformly by keeping its polarization, but with their energy distributed angularly on the surface of a plane perpendicular to the cylinder axis (see Figs. 2 and 3). The experimental data were plotted for all the polarization states reported here as normalized scattered Stokes vectors versus the scattering angle ($0° < \theta_s < 360°$) and also as points on the Poincarè sphere.

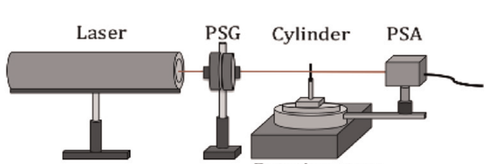

Fig. 1. Experimental setup employed for the measurement of the polarized light scattered by the metallic cylinder.

Fig. 2a shows the scattered energy s_o is distributed uniformly around $0° < \theta_s < 360°$ with almost pure s-polarization states, while there exist small contributions of linear −45° polarization (< 10%). Fig. 2b is a schematic representation of the energy distribution and the polarization states generated under the experimental conditions exposed here. The points on the Poincarè sphere, Fig. 2c, represent the scattered polarization states. Observe all of them are totally polarized (are on the unitary surface) and are basically located around the negative s_1 axis, which represents the s-polarization state.

On the other hand, Fig. 3 a shows how the incident p-polarized light is scattered uniformly as a p-polarized state in all the angular directions, except around $90° < \theta_s < 270°$, where elliptical left-handed polarization is slightly generated (< 10%). Fig. 3b represents the spatial-energy distribution with a scattered p-polarized state. Fig. 3c shows the scattered polarization states are located mostly around the positive s_1 axis, and some of them below the equator, on the lower hemisphere.

The results obtained when the +45° or −45° linear polarization states were used to illuminate the cylinder, are depicted in Figs. 4 and 5, respectively.

From Fig. 4(a) and (b), observe the incident +45° linear polarization state is scattered angularly as a point that describes a path on the Poincarè surface sphere, whose initial point is located near the negative s_2 axis (near to $\theta_s = 0°$) that moves gradually from the equator to the lower hemisphere, taking elliptical left-handed polarization states, passing close to the circular left-handed polarization pole at the negative s_3 axis, near to $\theta_s = 146.7°$. The point continues its displacement on the same hemisphere, now moving angularly faster, until it reaches a pure linear +45° polarization state on the positive s_2 axis, its antipodal point on the Poincarè sphere, at the direction of propagation ($\theta_s = 180°$). The point on the Poincarè sphere shows a tendency to follow a symmetric return to the negative s_2 axis, from $180° < \theta_s < 360°$. Note the denser distribution of points on the Poincarè sphere corresponds to the angularly slowly varying polarizations states outside the angular interval $145° < \theta_s < 225°$.

Note a similar behavior is presented when the incident beam has a linear −45° polarization (Fig. 5), with the exception that now the path on the Poincarè sphere begins at the positive s_2 axis located on the equator (near to $\theta_s = 0°$) and the elliptical polarization states move now on the upper hemisphere, passing close to the s_3 axis circular right-handed polarization state, around $\theta_s = 146.7°$ and later, arrives very close to the incident linear −45° polarization state ($-s_2$ axis), at $\theta_s = 180°$, the antipodal point of the s_2 axis. From $180° < \theta_s < 360°$ the path is closed by the moving point that returns to its original starting point at the equator, by following a symmetrical behavior.

Figs. 6 and 7 shows the results when the incident beam has a circular right- and a left-handed polarization state, respectively. The Fig. 6 shows the incident circular right-handed polarization state is scattered angularly, where each angular position has associated a point on the Poincarè sphere. In this case, the initial point is located at the negative s_3 axis, near to $\theta_s = 0°$. This point moves slowly towards its antipodal point, located at s_3, taking elliptical left-handed polarization states, passing close to the positive s_2 axis and crossing the equator (near to $\theta_s = 146.7°$). The point moves faster, taking on elliptical right-handed polarization states until it reaches the s_3 axis pole, at $\theta_s = 180°$. The symmetry of the graph after 180° shows the point describes the same path in reverse order, from the circular right-handed polarization,